The interfacial band bending induced the charge transfer regulation over Ag@ZIF-8@g-C_3N_4 to boost photocatalytic CO_2 reduction into syngas

Jia-Jia Li[a], Qing Zhang[a], Lin-Yan Zhang[b], Jian-Yong Zhang[b], Yufeng Liu[a], Na Zhang[a]*, Yong-Zheng Fang[a]

[a] *School of Materials Science and Engineering, Shanghai Institute of Technology, Shanghai, 201418, China*

[b] Schoolof Chemical and Environmental Engineering, *Shanghai Institute of Technology, Shanghai, 201418, China*

*Prof. Na Zhang, E-mail: nzhang@sit.edu.cn
Prof. Yong-Zheng Fang, E-mail: fyz1003@sina.com

1.1 Characterization

The crystal structures were investigated via Powder X-ray diffractometer (PXRD) on Bruker D8 Advance diffractometer using Cu Kα radiation. The scanning electron microscopy (SEM) (Hitachi S-4800 II) and transmission electron microscopy (TEM) (FEIJEM-2100) were applied to study the morphologies and size of samples. The adsorption-desorption isotherms for N_2 and CO_2 were obtained on a Micromeritics ASAP 2020 surface area analyzer. The chemical composition and states of samples were studied via X-ray photoelectron spectroscopy (XPS) on a Physical Electronics spectrometer (PHI-5702). The UV-vis spectra were obtained on a spectrophotometer (Agilent Cary 5000) using $BaSO_4$ as reference standard. The photoluminescence (PL) spectra were conducted on Varian Cary Eclipse spectrometer (Hitachi F-7000). Electron spin resonance (ESR) spectra were recorded on a Bruker ESP 300 Eelectron paramagnetic resonance spectrometer at room temperature with 5,5-dimethyl-1-pyrroline N-oxide (DMPO) and 2,2,6,6-Tetramethyl-1-piperidinyloxy (TEMPO) as spin trapping reagents.

1.2 Photocatalytic measurement

A standard three-electrode system was used to study the photo- and electrochemical behavior of the as-prepared photocatalysts. Ag/AgCl, Pt foil, and nickel foam electrode coated with photocatalyst were selected as standard electrode, counter electrode, and working electrode, respectively. The working electrodes were prepared following the steps: Firstly, the freshly-synthesized photocatalysts, super P, and Teflon emulsion were mixed evenly and the weight ratio was about 16:2:1. Then, the mixtures were added to the nickel foam (10×20 mm). A 300 W xenon lamp with a UV cut filter was used as the simulated sunlight source. The photocurrent response curves were recorded upon simulated visible-light irradiation on CHI instruments electrochemical workstation (model 660D) using 0.5 M Na_2SO_4 solution as electrolyte. The electrochemical impedance spectroscopy (EIS) tests were done using open circuit potential over the frequency range from 10^{-1} to 10^5 Hz. Linear sweep voltammetry (LSV) was carried out in Na_2SO_4 electrolyte (0.5 M) with a scan rate of 5 mV s^{-1}.

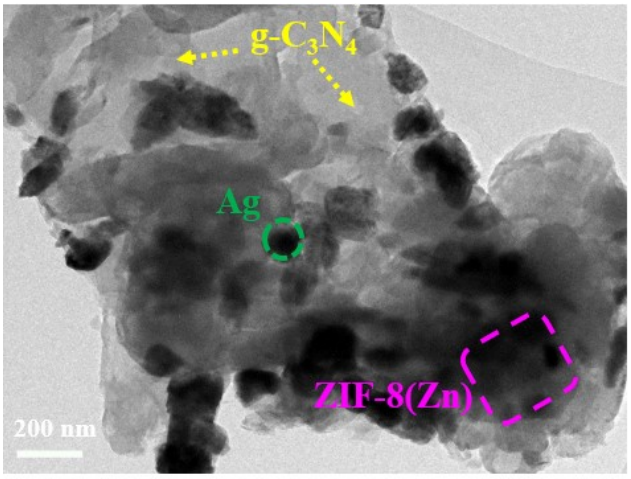

Fig.S1 The TEM image showing heterostructure of AZC-10 composite.

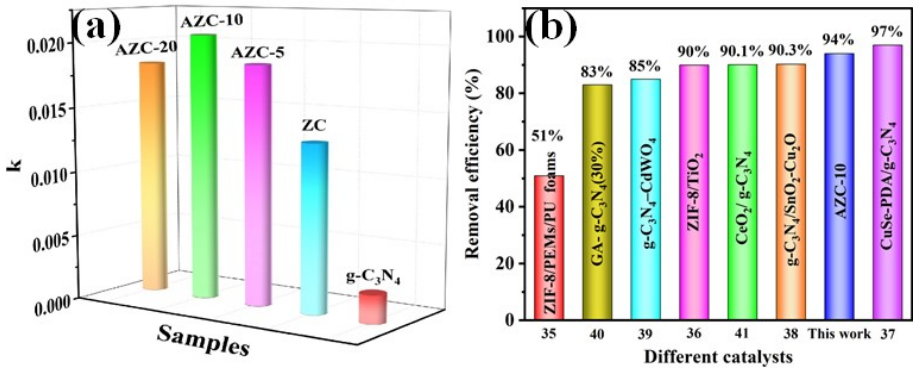

Fig.S2 (a) The comparison of kinetics for these photocatalysts, (b) the comparison of photodegradation efficiency for MB photodegredation.

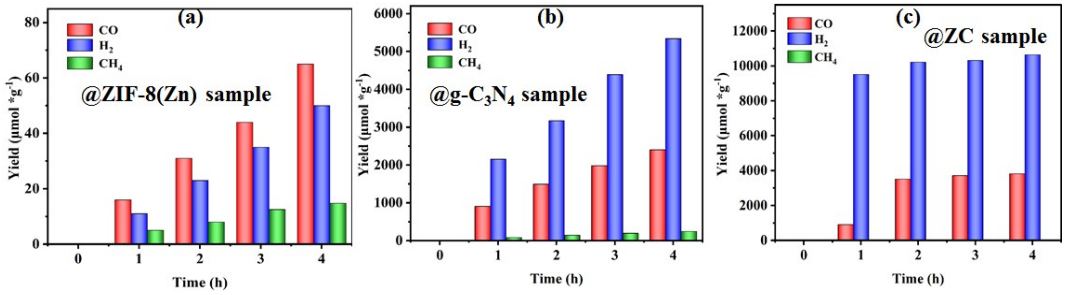

Fig.S3 The time-yield plot of syngas gas over ZIF-8(Zn) (a), g-C_3N_4 (b) and ZC catalyst (c).

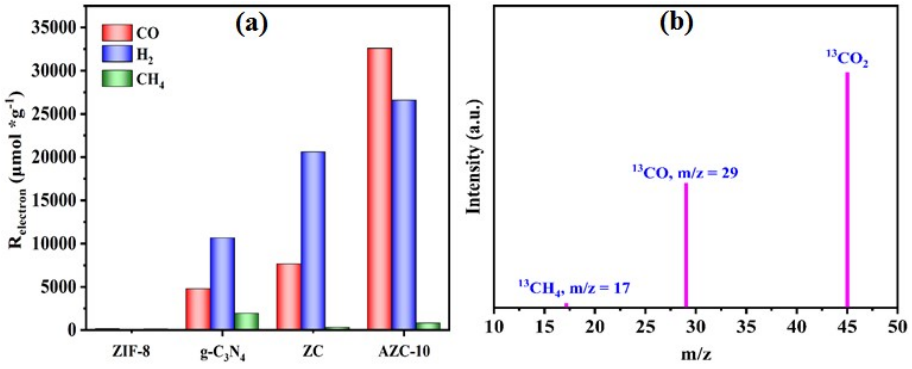

Fig.S4 (a) The corresponding electron consumption for the reduced products; (b) The Mass spectra of isotropic experiments with $^{13}CO_2$ as gas source.

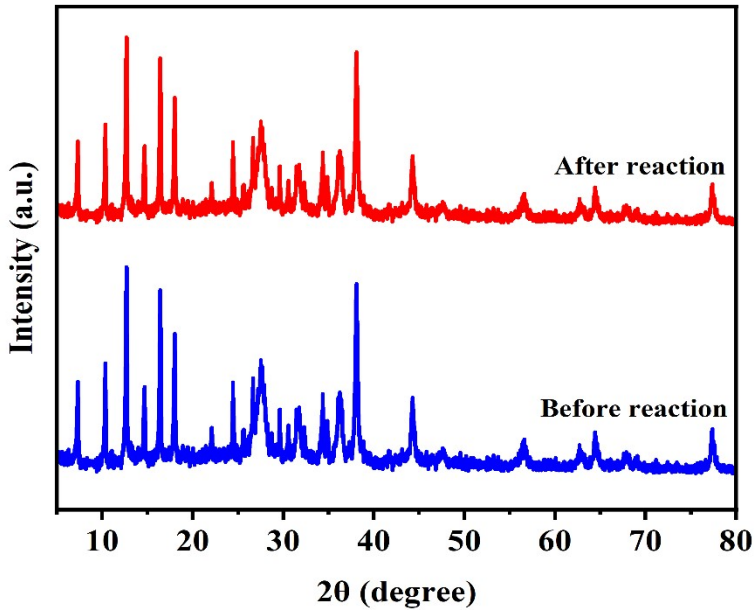

Fig.S5 The PXRD patterns of AZC-10 before and after CO_2 reduction reaction

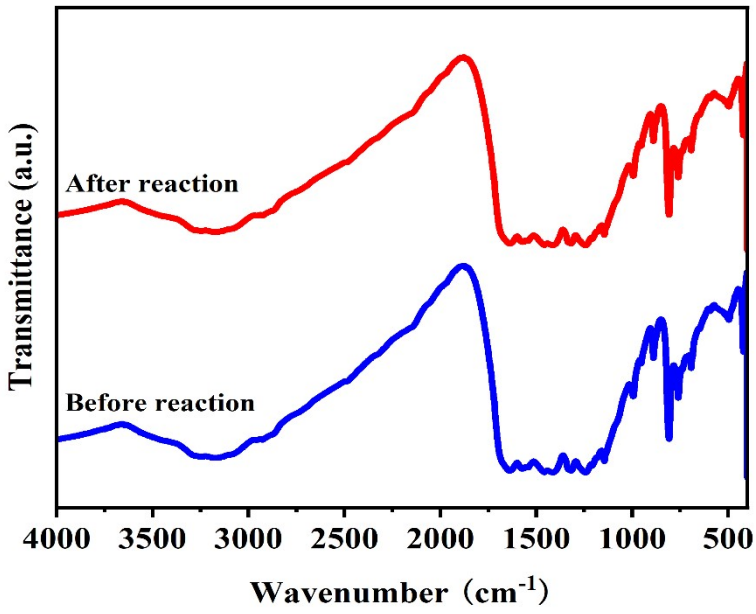

Fig.S6 The FT-IR spectra of AZC-10 before and after CO_2 reduction reaction

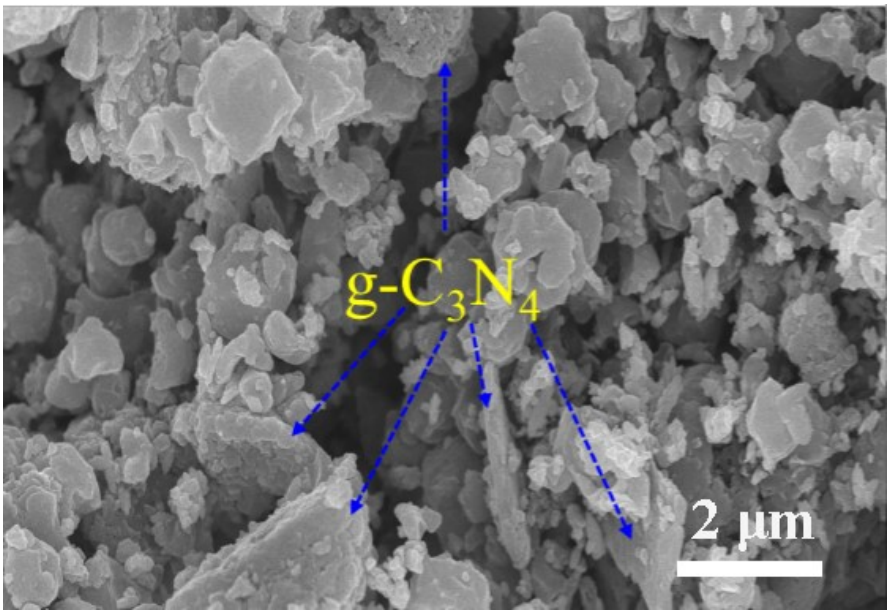

Fig.S7 SEM image of AZC-10 catalyst after CO_2 photoreduction reaction.

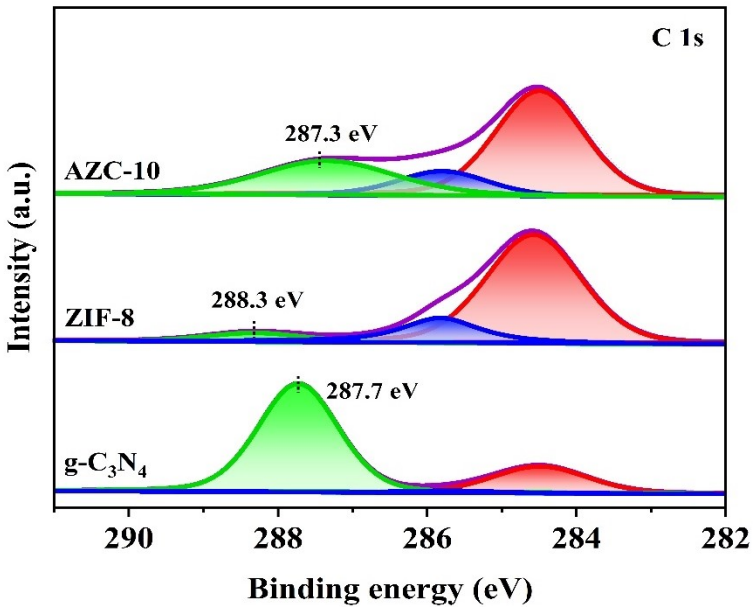

Fig.S8 High-resolution XPS spectra of C1s.

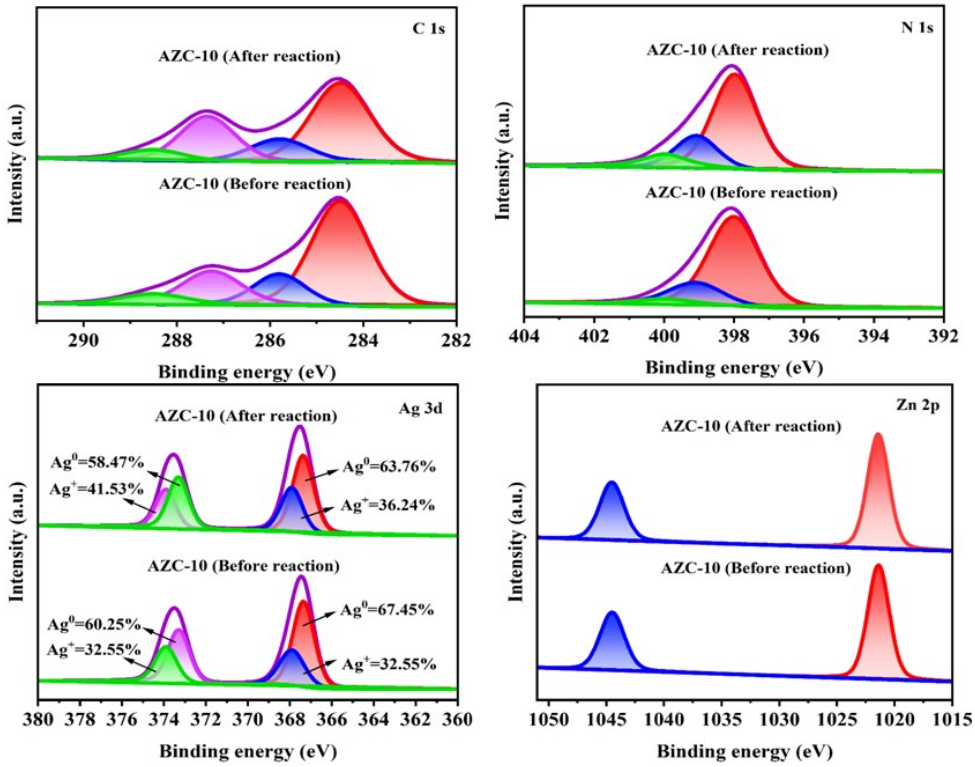

Fig.S9 The comparison of XPS spectra of C 1s, N 1s, Ag 3d and Zn 2p over AZC-10 photocatalyst before and after reaction.

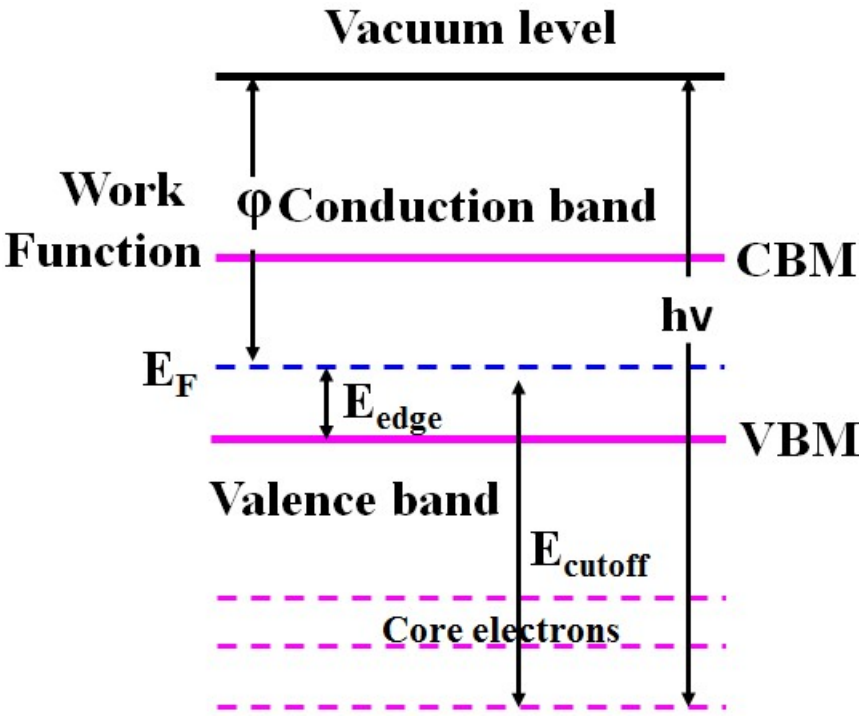

Fig.S10 The E_{VBM} and E_{CBM}) of each single material (vs. vacuum level).

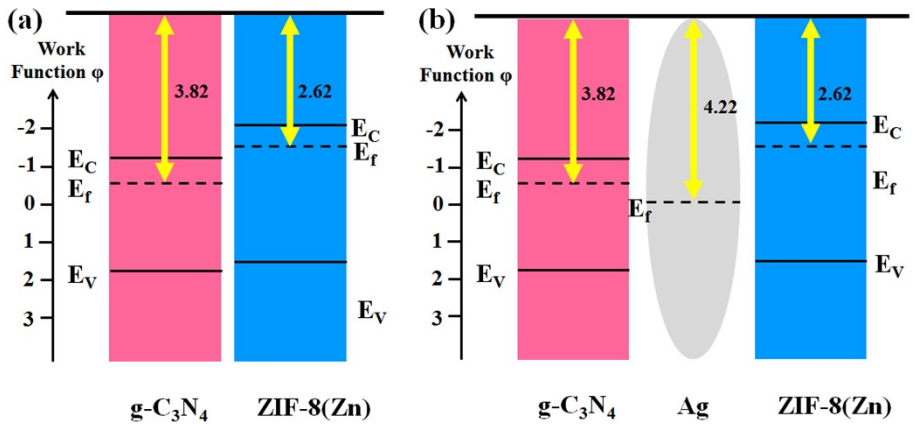

Fig.S11 the work functions Φ of g-C_3N_4 and ZIF-8(Zn) according to UPS.

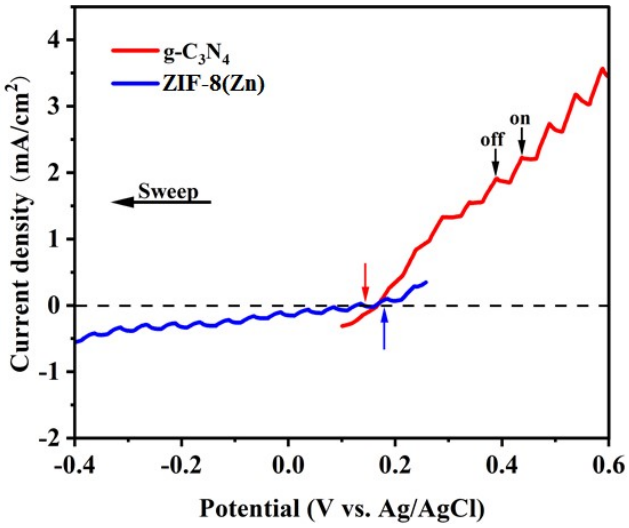

Fig.S12 The current-potential curves of g-C_3N_4 and ZIF-8(Zn) under visible light (λ > 420 nm) irradiation.

Table S1 The S_{BET}, V_t obtained from N_2 isotherm and CO_2 uptake capacities of various samples.

Sample	S_{BET} (m^2/g)	V_t (cm^3/g)	Maximum CO_2 uptake (mmol/g)
g-C_3N_4	12.6	0.096	0.292
ZIF-8(Zn)	1296.6	0.754	0.497
ZC	1013.4	0.588	1.24
AZC-10	947.7	0.517	1.17

Table S2 Comparison of photodegradation performances for over various photocatalysts.

Catalysts	Dosage (g/L)	C_0 of MB (mg/L)	Light sources	Time (min)	Removal efficiency (%)	References
ZIF-8/PEMs/PU foams	-	20	UVC irradiation	180	51	1
ZIF-8/TiO_2	0.5	10	Xenon lamp	40	90	2
CuSe-PDA/g-C_3N_4	-	50	visible-light	60	97	3
g-C_3N_4/SnO_2-Cu_2O	0.5	30	simulated sunlight	100	90.3	4
g-C_3N_4-$CdWO_4$	2	1	visible light	75	85	5
GA-g-C_3N_4 (30%)	0.2	20	visible light	180	83	6
CeO_2/g-C_3N_4	0.5	10	UV lamp	180	90.1	7
AZC-10	0.167	20	Simulated solar	120	94	This work

References

[1] P. Plengplung, C. Ratanatawanate, S. T. Dubas, Improved stability of zeolitic imidazolate framework-8 photocatalytic coating on polyurethane foam via polyelectrolyte multilayer surface modification, Colloids and Surfaces A: Physicochemical and Engineering Aspects, 629(2021)127415.

[2] W.-L. Zhong, C. Li, X.-M. Liu, X.-K. Bai, G.-S. Zhang, C.-X. Lei, Liquid phase deposition of flower-like TiO_2 microspheres decorated by ZIF-8 nanoparticles with enhanced photocatalytic activity, Micro. Meso. Mater. 306 (2020) 110401.

[3] M. Bai, C. Xu, X. Huang, H. Yin, J. Wan, Preparation of CuSe-PDA/g-C_3N_4 and its visible-light photocatalytic performance to dye degradation, Environ. Sci. Pollut. Res. 28 (2021) 3465-3474.

[4] R. S. Sutar, R. P. Barkul, S. D. Delekar, M. K. Patil, Sunlight Assisted Photocatalytic Degradation of Organic Pollutants Using g-C_3N_4-TiO_2 Nanocomposites, Arab. J. Chem. 13(4) (2020) 4966-4977.

[5] S. P. Keerthana, R. Yuvakkumar, P. S. Kumar, G. Ravi, S. I. Hong, D. Velauthapillai, Investigation of pure and g-C_3N_4 loaded $CdWO_4$ photocatalytic activity on reducing toxic pollutants, Chemosphere doi.org/10.1016/j.chemosphere.2021.133090

[6] J. Y. Zhang, S. H. Zhang, J. Li, X.-C. Zheng, X.-X. Guan, Constructing of 3D graphene

aerogel-g-C_3N_4 metal-free heterojunctions with superior purification efficiency for organic dyes, J. Mol. Liq. 310 (2020) 113242.

[7] X. Wei, X. Wang, Y. Pu, A. Liu, C. Chen, W. Zou, Y. Zheng, J. Huang, Y. Zhang, Y. Yang, M. Naushad, B. Gao, L. Dong, Facile ball-milling synthesis of CeO_2/g-C_3N_4 Z-scheme heterojunction for synergistic adsorption and photodegradation of methylene blue: Characteristics, kinetics, models, and mechanisms, Chem. Eng. J., 420 (2021) 127719.